Penerbit Akademia Baru

Journal of Research in Nanoscience and Nanotechnology

Journal homepage:
http://akademiabaru.com/submit/index.php/jrnn/index
ISSN: 2773-6180

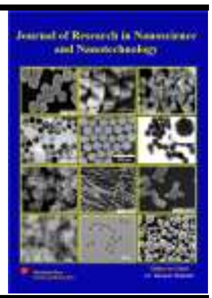

Exact Analysis on Heat and Mass Flow Rates Computations over a Ramping Wall Boundary with C_8H_{18}/Al_2O_3 Based MHD Nanofluid Flow Past a Vertical Surface

Kayalvizhi Joshua [1], and Vijaya Kuma Avula Golla [1,*]

[1] Department of Mathematics, School of Advanced Sciences Vellore Institute of Technology, Vellore-632014, India
* Correspondence: vijayakumarag@vit.ac.in
https://doi.org/10.37934/jrnn.15.1.122

ABSTRACT

An exact solution is derived for parabolic equations with partial differentials for the analysis of the ramping wall boundary of a nanofluid flow, suspended aluminium oxide nanoparticle in the Gasoline influenced by magnetic and gravitational forces in a semi-infinite flow region using integral transform method. Rosseland's approximation is used for radiative heat flow in the energy equation, whereas Bousinessq's approach is used in the momentum equation. Fluid temperature, species concentration, and transport are solved using Heaviside, exponential and complementary error functions; friction drag, heat and mass transfer rates are solved using Gaussian error functions. Numerical calculations have been carried out for rate of heat transmission and Sherwood number is swotted to put in the form of tables while the temperature, transport and species concentration are graphically exhibited. Higher radiation parameters lead to an increase in fluid temperature. The velocity boundary layer is decreased by the magnetic field and the opposite behaviour observed in porous media parameters. The heat transfer rate drops as Prandtl number and radiation parameter grows for both ramping and isothermal situations, whereas increases when time, volume fraction and heat source parameter increase. While increasing the schimidt number, mass transfer increase magnitudely for both cases.

Keywords:
Ramped wall conditions; gasoline; aluminium oxide; method of integral transform; radiative heat flux; magnetic induction

Received: 27 Jan 2025	Revised: 20 Feb. 2025	Accepted: 25 Mar. 2025	Published: 30 Apr. 2025

1. Introduction

Nanotechnology is gaining popularity as a result of its important function of improving the heat capacity of liquids by boosting heat and mass transfer rates. Due to its wide variety of applications in biomedicine, heat exchangers, electronic device cooling, double windowpane, food, transportation and other fields, the idea of nanofluids has become a more expansive topic for the research community in recent years. In order to improve the heat capacity of common fluids like water, kerosene, and motor oils etc., we must add various types of nanoparticles to the base fluids, such as graphene, silica, silver, gold, copper, alumina, carbon nanotubes, and so on. These nanofluids were introduced by Choi and Eastman [1]. A large number of research papers have been published in the literature that deals with improving the thermal conductivity of base fluids by adding various types of nanoparticles. Makinde has investigated the modelling of nanofluid flow [2]. Eastman *et al.,* [3,4] reported that when CuO nanoparticles with a volume fraction of 5 % were introduced to the base fluid (water), the heat conduction of the considered base fluid increases at most 0.6. Whereas 1 % of copper nanoparticles was introduced into ethylene glycol or oil, 40 % thermal conductivity was increased. This is due to metals have three times the thermal conductivity of general fluids, this one is permissibles to carry out heat transmission with mix up of two constituents that act to be a fluid matter but possesses the thermal conductivity of metals. Nanofluids (water-Al2O3) in a two-dimensional horizontal pipe have been studied by Elfaghi *et al.,* [5] to increase heat transfer. Nura Muaz Muhammad *et al.,* [6] did research on a numerical investigation on the combined effect of aluminum-nitride/water nanofluid with different mini-scale geometries for passive hydrothermal augmentation

Many researchers are interested in discovering MHD in the combination of heat and mass transport with radiation impact due to its vast variety of applications. It is used in astrophysics and geophysics to investigate stellar and solar structures, as well as radio transmission via the ionosphere. It has uses in engineering, such as MHD pumps and MHD bearings. Mass transfer is a well-known phenomenon in stellar structure theory, and observable consequences may be seen on the surface of the sun. The thermal physics of hydromagnetic issues with mass transport has a lot of applications in power engineering. Thermal radiation plays an immense role in surface heat transfer, it is used in manufacturing, the design of dependable equipment, nuclear power plants, gas turbines, aeroplanes, missiles, satellites, space vehicles, space technologies, and procedures involving high temperatures. In the medical field, lukewarm radiation is in high demand. The impact of thermal radiation with doubling diffusion has been an important research issue for many experimenters because of its use in medical therapy. Infrared radiation is a common kind of heat treatment that is used in many different parts of the human body it is produced by oscillations in the electromagnetic field. Radiative heat transfer allows electromagnetic waves to carry vitality. It's a link between visible brightness and microwaving. It can help with a variety of skin issues. The wavelength of radiation penetrating the skin was determined by its radiating structure, vascularity, and pigmentation. Heat treatment is aided by infrared radiation, which warms the afflicted area's blood capillaries directly. It improves the body's blood flow, which helps to prevent infection in superficial wounds. It also draws attention to white blood cells while removing waste products.

Makinde *et al.,*[7] investigated the flow and heat transmission properties of an MHD nanofluid. Aly and Chamkha [8] investigated the numerical analysis of a nanofluid flow by a mode of natural convection in a steady state containing nanoparticles through upward porosity plate under the action of magnetism. Thermal production or shrink, influenced by the magnetic force of action the thermal radiating processes identified by Nayak *et al.,* [9] were used to study 3D natural convection magnetohydrodynamic nanofluid flow through porous linear stretching surfaces. An analysis of radiation impacts on magnetohydrodynamics on the convective flow of nanofluids traversing a vertical stretching sheet was carried out by Turkyilmazoglu and Pop [10]. To investigate the effect of the radiative flux of heat on the thermal process and the flow of magnetic nanofluid, Sheikholeslami *et al.*, [11] developed a two-phase model. A study conducted by Chamkha [12] investigated the fluid flow by a convective mechanism at a sloping surface nearer to the porous zone. In addition, Chamkha

[13] explored the source of heat or sink impact in a magnetic fluid along with a magnetohydrodynamic flow over an accelerated porosity surface. Unsteadiness, magnetic fluid flow was seen on a motion of an up straight plate with nanofluid by M. Veera Krishna *et al*. [14], and a heat source or shrink effects were discovered. J. Prakash *et al.,* [15] explored the role of MHD free convection flow using a transversely applied magnetic field combined with a temperature gradient and mass diffusion in a porous medium. Non-Darcian natural convection flow of viscoelastic fluids between vertical plates has been addressed by Ewis *et al.,* [16]. Adnan Ashgar *et al.,* [17] computes a three-dimensional hybrid nanofluid flow across a stretching/shrinking sheet. Nurul Shahirah Mohd Adnan *et al.,*[18] examines the stability of a dual solution to the stagnation-point slip flow issue across a stretching or shrinking cylinder. Ansys Fluent software is used by Azraf Azman *et al.,* [19] to simulate the flow of hybrid nanofluids in a straight tube. Fluid flow and heat transfer toward a moving flat plate are studied by Mohammad Ferdows *et al.,* [20] in a stable free convective boundary layer. Shervin Sharafatmandjoor *et al.,* [21] tested the Influence of Imposition of Viscous and Thermal Forces on Dynamical Features of Microorganism Swimming in Nanofluids. Waqar Ahmed *et al.,*[22] evaluated Metal Oxide and Ethylene Glycol Based Well Stable Nanofluids for Mass Flow in a Covered Pipe.

With the magnetic field consideration, Hamad *et al.,* [23] inspected the features of spontaneously the mechanism of convective nanofluid flow along with the bounded vertical plate. The transport of nanofluid across an endless upward-directed plate, studied by Das and Jana [24]. Unsteady flow through an accelerated vertical plate embedded in pores material was studied by Hussain *et al.,* [25]. Sheikholeslami *et al.,* [26] examined convective MHD. Al_2O_3–H_2O nanofluid transport. Das *et al.,* [27] demonstrated nanofluid transport and heat transport utilising magnetic Nano-fluid flow over a vertical stretching sheet. Chamkha and Aly reported on MHD convective nanofluid flow across a vertical plate in the presence of a heat source/sink [28]. The stagnation point flow of nanofluids was investigated studied by Soomroet *et al.,* [29] for heat generation/absorption and radiation impacts. For mixed free and forced convection flow, Hayat *et al.,* [30] studied the ability of an Oldroyd-B fluid in view of thermal source/shrink. Casson-type nanofluid, researched by Khan *et al.,* [31] within the presence of magnetic force and source and sink of heat radiative effects. E Kumaresan *et al.,* [32] researched to examine the effects of absorption of radiation which is chemically reacting in a nanofluid flow of with CuO-H_2O and MgO-H_2O nanoparticle combinations across a stretched sheet in pores material with source or shrink of heat. Rahimah Mahat *et al.,*[33] calculate the effect of viscous dissipation by a sodium carboxymethyl cellulose (CMC-water) nanofluid containing copper nanoparticles at ambient temperature with convective boundary conditions.Mohamad Hafzan Mohamad Jowsey *et al.,* [34] examine the heat and flow profile of nanofluid flow within a multilayer microchannel heat sink.T. W. Akaje *et al.,*[35] studied the impact of nonlinear radiative heat on the species heat transfer of an MHD Casson nanofluid flow with a Thompson and Troian boundary condition.By using pure water and Fe_3O_4-H_2O as working fluids, Nor Azwadi Che Sidik[36] performed numerical analysis on the three-dimensional rectangular silicon microchannel heat sink (MCHS). According to Abdolbaqi Mohammed Khdher[37], three different nanofluids in a fully developed turbulent flow inside a long horizontal duct are being studied for pressure drop as well as secondary flow and convection heat transfer phenomena

Many studies are exploring ramped temperature profiles. The term "ramped temperature" refers to the fact that, for a period of time, the rate of change in temperature. But it should be remembered that the time domain for ramped profiles alter from substance to substance based on the material's specified heat capacity. Varying ramped curves of temperature may be found in real-world applications such as building air conditioning systems, thermal management of nuclear operations, processes of warming and freezing, designing of devices, material processing of phase transition, thin-film photovoltaic device manufacturing, and heat exchangers. MHD natural convection flows with mass and heat transfer past an impulsively moving plate with ramping temperature was studied by Siva Reddy Sheri *et al.,* [38]. Convective mode of heat transfer besides mass transfer has been studied by Seth *et al*., [39] in which Hall currents, rotation, radiation, and heat absorption are all considered. Magnetic convective flow transport on a moving normal plate was scrutinized by Seth *et al*. [40] to notice the impact of Hall currents.

Unsteady Newtonian fluid flow across a suddenly started infinitely long upright plate was originally addressed by Ahmed and Dutta [41] using ramping wall velocity and temperature. Chang *et al*. performed a study to reveal the ramping boundary temperatures on convective viscous fluid transport [42]. According to Kataria *et al.,* [43] analysed the importance of dufour and parabolic motion impacts over an infinitely upright surface, observed the unsteadiness, through the mode of convection, a second-grade fluid, in a porosity region with ramping wall temperatures and concentrations are studied for heat production and absorption. A computational study of convective magnetohydrodynamic heat flow by radiation over an impulsive plate with ramping fluid temperature was undertaken by Shri Siva Reddy *et al*., [44], and Seth *et al.,* [45] developed an even more detailed study of ramping wall temperature. The influence of fluid temperature due to ramp over a plate boundary, the heat transmission is due to convection is investigated by Narahari *et al*., [46]. In their work, Seth *et al*., [47-48] investigated the mass and heat transfer properties of materials under a variety of physical conditions such as chemical reaction, Darcy's law and Hall current. While taking Hall current into consideration, M. VeeraKrishna *et al.,* [49] examined the thermo-diffusion and heat injection/suction impact in an unstable magnetic convective flow with radiation influence by chemical reaction of a type of second-grade fluid near an endless vertically projected plate. Analysis of the unstable magnetic convective flow of Casson fluid along the surface of the upright plate moving with exponential acceleration influence by a first-order chemical reaction with heat source/sink via embedded porosity zone was explored by Kataria *et al.,* [50,52]. Very recently, under ramping temperature and velocity circumstances at the wall, researchers V. Talha Anwar *et al*., [51] evaluated the unstable Casson MHD fluid flow through an endless vertical plate. Chamkha and Veera Krishna and [53] examined, a second-grade fluid, in a permeable region using ramped thermal conditions. Under chemical reaction and heat source impact, Ansab Azam Khan *et al*., [54] analyze the heat and mass transfer of MHD micropolar fluid flow including twofold stratification via a stretching/shrinking vertical sheet. This CFD research of convective heat transfer in a micro-pipe with mixed constant wall temperature and heat flux wall boundary conditions was carried out by Amjad Ali Pasha *et al.,* [55]. Free convection flow of Jeffrey nanofluid across a horizontal circular cylinder with viscous dissipation effect, as shown by Syazwani Mohd Zokri *et al.,* [56].

To the best knowledge of the author’s, an unstable incompressible MHD nanofluid flow suspended boron and aluminium oxide nanoparticles in the base fluid that is exposed to ramped velocity, ramped temperature, and ramped wall concentration conditions at a vertical edge in a porous zone field has not yet been addressed. In addition, the radiation and heat generation/absorption are included in heat transfer in order to assess their relevance in the heat transfer process. Integral transformation techniques are applied to execute the results of modelled concentration, energy, and momentum equations, and they are implemented. Finally, with the use of tables and graphs, the physical characteristics of the necessary parameters are investigated.

2. Geometry and Formulation of the Problem

The rectilinear system of coordinates is cogitated. The plate is located at the origin along the y-axis and filled with the fluid in plane quadrant. An infinite plate is surrounded by the $x'-$axis in an upward direction against to axis y' and the semi-region of $x'y'-$plane filled with nanofluid contains boron and aluminium oxide nanoparticles in a pores zone. In the initial state ($t' \le 0$) the plate surface and nanofluid overall the region is in static condition and after elapsing certain time ($t' > 0$), the plate is given a ramped motion $u' = u_0 t'/t_0$ at that instant, the plate temperature ramped $T' = T_0' + (T_w' - T_0')t'/t_0$ with increasing levels of concentration $C' = C_0' + (C_w' - C_0')t'/t_0$ all within the range of time $0 < t' \le t_0$, after the certain characteristic time (t_0) plate velocity, temperature and concentration reaches to the isothermal state of condition. The effect of Lorentz force $\overline{J} \times \overline{B}$ is acting in $x'-$momentum, such that the magnetic force of lines impact developed by the momentum of electrified conductive fluid is ignorable. This assumption gives rise to as the magnetic Reynolds number is too tiny which is generally occurs in the case of aerodynamic applications. Since no outside electrical field is introduced and the effect of polarisation of the ionised field is neglected it is also assumed that the field of electricity $\overline{E} = 0$. Under the above assumption the components of electromagnetic induction are given by $B_x = 0, B_y = B(x)$ the ponderomotive $\overline{F} = \overline{J} \times B/\sigma$ reduces to $F_x = \left(-\sigma B_0{}^2(x)/\rho\right)u, F_i = 0$ while radiative energy flux and a heat source are encountered in the energy equation. The buoyant force is the essential mechanism in driving the fluid through gravity is pulling down. Since the plate is taken infinite length, the boundary layer thickness is considerably small when compare, hence all the flow fields only function of one special coordinate and with respect to time. The fluid is supposed to be grey in colour and capable of both absorbing and emitting radiation, although it is not considered to be a scattering medium. The governing equations of momentum, energy, and concentration describing the fluid flow phenomena are formulated accordingly to simplify pressure gradient and body force in the Navier-Stokes equation, while the approximation of Rosseland was applied to approximate the thermal equation in radiative terms and presented in dimensionless form as follows:

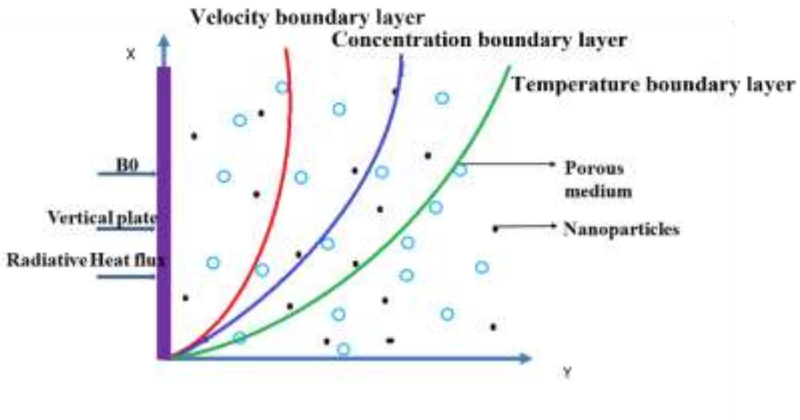

Fig. 1. Physical representation of the problem

As a result of the above analysis, the flow is governed by [53] such as,

$$\rho_{nf}\frac{\partial u'}{\partial t'} = \mu_{nf}\frac{\partial^2 u'}{\partial y'^2} + g(\rho\beta)_{nf}\left(T' - T_0{}'\right) + g(\rho\beta)_{nf}\left(C' - C_0{}'\right) - \sigma_{nf}B^2 u' - \frac{\mu_{nf}\Psi}{k}u \tag{1}$$

$$(\rho cp)_{nf}\frac{\partial T'}{\partial t'}=k_{nf}\frac{\partial^2 T'}{\partial y'^2}-\frac{\partial q_r'}{\partial y'}-Q'\left(T'-T_0'\right) \tag{2}$$

$$\frac{\partial C'}{\partial t'}=D\frac{\partial^2 C'}{\partial y'^2} \tag{3}$$

The adequate corresponding initial and boundary conditions are given by [53,57]

$$T'=T_0',\ C'=C_0',\ u'=0 \text{ for } 0\le y',t'>0 \tag{4}$$

$$u'=\begin{cases} u_0'\dfrac{t'}{t_0'} & \text{if } 0<t'<t_0 \\ u_0' & \text{if } t'\ge t_0 \end{cases} \quad \text{at } t'\ge 0 \text{ and } y'=0 \tag{5}$$

$$T'=\begin{cases} T_0'-(T_0-T_w)\dfrac{t'}{t_0'} & \text{if } 0<t'<t_0 \\ Tw' & \text{if } t'\ge t_0 \end{cases} \quad \text{at } y'=0,\ t'\ge 0 \tag{6}$$

$$C'=\begin{cases} (C_w-C_0)\dfrac{t'}{t_0'}+C_0' & \text{if } 0<t'<t_0 \\ Cw' & \text{if } t'\ge t_0 \end{cases} \quad \text{at } y'=0,\ t'\ge 0 \tag{7}$$

$$\text{as } y'\to\infty \text{ when } t'\ge 0 \quad u'\to 0,\quad T'\to T_0',\quad C'\to C_0' \tag{8}$$

Famous astrophysicist Svein Rosseland provided an approximation of radiation flux for a boundary layer that is optically thick as the following:

$$\frac{\partial q_r'}{\partial y'}=-4a^1\sigma^1\left(T_\infty-T^4\right) \tag{9}$$

When expanding Taylor's series T^4 on the point T_∞ and omitting the terms from the second degree onwards, it has the form of:

$$T^4\cong(4T-3T_\infty)T_\infty^{\ 3} \tag{10}$$

Plugging Eq. (9) along with Eq. (10) in Eq. (3) yields

$$(\rho cp)_{nf}\frac{\partial T'}{\partial t'}=\left(k_{nf}+\frac{16\sigma_1 T^3_{\ \infty}}{3k_1}\right)\frac{\partial^2 T'}{\partial y'^2}-Q'\left(T'-T_0'\right) \tag{11}$$

The physical properties of nanofluid provided by [38] as follows:

$$\mu_{nf}=(1-\phi)^{-2.5}\mu_f\ ,\ \rho_{nf}=\phi\rho_s+\rho_f(1-\phi)\ ,\ (\rho cp)_{nf}=(\rho cp)_s\phi+(1-\phi)(\rho cp)_f$$

$$(\rho\beta)_{nf}=\phi(\rho\beta)_s+(1-\phi)(\rho\beta)_f\ ,\ \sigma_{nf}/\sigma_f=\left[1+\frac{3(\sigma-1)\phi}{(\sigma+2)-\phi(\sigma-1)}\right],\quad \sigma=\frac{\sigma_s}{\sigma_f}$$

$$knf=k_f\left[\frac{(k_s+2k_f)-2\phi(k_f-k_s)}{(k_s+2k_f)+\phi(k_f-k_s)}\right]$$

The base fluid and nanoparticles are denoted by the subscripts f and s, respectively, while the nanoparticles volume concentration is denoted by ϕ

Together with the corresponding parameters

$$y=\frac{u_0 y'}{\gamma_f},\ t=\frac{u_0{}^2 t'}{\gamma_f},\quad u=\frac{u'}{u_0},\ \theta=\frac{T'-T_w'}{T_w'-T_0'},\ C=\frac{C'-C_0'}{C_w'-C_0'},\ t_0=\frac{\gamma_f}{u_0{}^2}$$
$$pr=\frac{\mu cp}{k},\quad M^2=\frac{\sigma B_0{}^2}{\rho u_0{}^2}t_0,\quad \frac{1}{K}=\frac{\gamma_f{}^2\psi}{ku_0{}^2},\quad Nr=\frac{16\sigma_1 T_\infty{}^3}{3k_f k_1} \tag{12}$$
$$Gr=\frac{\beta g\gamma\left(T_w'-T_0'\right)}{u_0{}^3},\quad Gm=\frac{\beta g\gamma\left(C_w'-C_0'\right)}{u_0{}^3},\quad sc=\frac{\gamma}{D}$$

Eqs. (1), (2), and (11) are transformed into

$$\frac{\partial u}{\partial t}=a_1\frac{\partial^2 u}{\partial y^2}+a_2(Gr\theta+GmC)-\left(a_3M^2+\frac{a_1}{K}\right)u \tag{13}$$

$$\frac{\partial\theta}{\partial t}=a_4\frac{\partial^2\theta}{\partial y^2}-a_5\theta \tag{14}$$

$$\frac{\partial C}{\partial t}=\frac{1}{sc}\frac{\partial^2 C}{\partial y^2} \tag{15}$$

where

$$z_1=\left[1-\phi+\phi\frac{(\rho)_s}{(\rho)_f}\right],\ z_2=\left[1-\phi+\phi\frac{(\rho\beta)_s}{(\rho\beta)_f}\right],$$

$$z_3=\left[1-\phi+\phi\frac{(\rho cp)_s}{(\rho cp)_f}\right],\ z_4=\left[1+\frac{k_s-2\phi\left(k_f-k_s\right)+2k_f}{k_s+\phi\left(k_f-k_s\right)+2k_f}\right],$$

$$z_5 = \left[1 + \frac{3(\sigma - 1)}{(\sigma + 2) - (\sigma - 1)}\right]$$

$$a_1 = \frac{\mu_f}{(1-\phi)^{2.5} z_1} \ , \ a_2 = \frac{z_2}{z_1} \ , \ a_3 = \frac{z_5}{z_1} , \ a_4 = \frac{1}{z_3 pr}(z_4 + Nr) \ , \ a_5 = \frac{Q}{z_3}$$

The boundary conditions are taken into consideration

$$u = T = C = 0 \qquad y \geq 0 \quad , \ t < 0 \tag{16}$$

$$u = \begin{cases} t & if \ \ 0 < t \leq 1 \\ 1 & if \ \ t > 1 \end{cases} \qquad at \ \ y = 0, \ t > 0 \tag{17}$$

$$T = \begin{cases} t & if \ \ 0 < t \leq 1 \\ 1 & if \ t > 1 \end{cases} \qquad at \ \ y = 0, \ t > 0 \tag{18}$$

$$C = \begin{cases} t & if \ \ 0 < t \leq 1 \\ 1 & if \ \ t > 1 \end{cases} \qquad at \ \ y = 0, \ t > 0 \tag{19}$$

for $t > 0$, as $y \to \infty$, the fluid components leads to $u \to 0$, $T \to 0$, $C \to 0$ (20)

3. Solution of the Problem

The terminology specifies the physical factors that have shown themselves. The equations governed by the flow in non-dimensional form, listed from (13) to (15), solved with associated initial condition, along with the conditions defined at boundaries, from (16) to (20), by the usual Integral transform technique, and the resultant solutions are derived in form of exponential function, and Gaussian probability density function and unit step functions.

$$\bar{u}(y,s) = \left\{ \begin{array}{l} \left(\frac{1-e^{-s}}{s^2}\right) e^{-y\sqrt{\beta s + \beta a^*}} + \left(1-e^{-s}\right)\left[\frac{b}{ds^2} - \frac{b}{d^2 s} + \frac{b}{d^2(s+d)}\right]\left(e^{-y\sqrt{\beta(s+a^*)}} - e^{-y\sqrt{\alpha(s+a_5)}}\right) + \\ \left(1-e^{-s}\right)\left[-\frac{b1}{d1s^2} - \frac{b1}{d1^2 s} + \frac{b1}{d1^2(s+d1)}\right]\left(e^{-y\sqrt{\beta(s+a^*)}} - e^{-y\sqrt{ssc}}\right) \end{array} \right\}$$

(21)

$$\bar{\theta}(y,s) = \exp(-y\sqrt{\alpha s + \alpha a_5})\left(\frac{1 + (-e^{-s})}{s^2}\right) \tag{22}$$

$$\bar{C}(y,s) = \exp(-y\sqrt{ssc})\left(\frac{1 - e^{-s}}{s^2}\right) \tag{23}$$

where

$$\alpha=\frac{1}{a_4}\ ,\quad \beta=\frac{1}{a_1}\ ,\ a^*=a_3M^2+\frac{a_1}{K}\ ,\quad a_6=\frac{a_2}{a_1}\ ,\quad b=\frac{Gra_2}{(a_1\alpha-1)}\ ,\ b_1=\frac{Gma_2}{(a_1sc-1)}\qquad d=\frac{\alpha a_5-a^*}{\alpha-1}\ ,$$

$$d_1=\frac{a^*}{(sc-1)}$$

For inverse Laplace transform of Eqs. (21) – (23) we get

$$u(y,t)=\begin{bmatrix}\left(1+\frac{b}{d}-\frac{b_1}{d_1}\right)F-\left(1+\frac{b}{d}-\frac{b_1}{d_1}\right)F_1\ H(t-1)+\left(\frac{b}{d^2}\right)G-\left(\frac{b}{d^2}\right)G_2\ H(t-1)-\left(\frac{b}{d^2}\right)G_1+\left(\frac{b}{d^2}\right)G_3\,H(t-1)\\ +\left(\frac{b_1}{d_1^{\,2}}\right)I-\left(\frac{b_1}{d_1^{\,2}}\right)I_2H(t-1)-\left(\frac{b_1}{d_1^{\,2}}\right)I_1+\left(\frac{b_1}{d_1^{\,2}}\right)I_3H(t-1)-\left(\frac{b}{d^2}\right)R+\left(\frac{b}{d^2}\right)R_3\,H(t-1)+\left(\frac{b}{d^2}\right)R_1\\ -\left(\frac{b}{d^2}\right)R_4\,H(t-1)-\left(\frac{b}{d}\right)R_2+\left(\frac{b}{d}\right)R_5\ H(t-1)-\left(\frac{b_1}{d_1^{\,2}}\right)J+\left(\frac{b_1}{d_1^{\,2}}\right)J_3\,H(t-1)+\left(\frac{b_1}{d_1^{\,2}}\right)J_1\\ -\left(\frac{b_1}{d_1^{\,2}}\right)J_4\,H(t-1)+\left(\frac{b_1}{d_1}\right)J_2-\mathrm{H(t-1)}\left(\frac{b_1}{d_1}\right)J_5\end{bmatrix}\tag{24}$$

$$\theta(y,t)=R_2(y,t)-H(t-1)R_5\tag{25}$$
$$C(y,t)=J_2(y,t)-H(t-1)J_5$$

4. Solution in the Case of Isothermal Plate with Uniform Boundary

These solutions may beneficial to compare fluid transport with uniform temperature along an upright surface with, uniform transport and concentration to emphasise the influence of ramping temperature, velocity and species concentration on flow transport phenomena. The results of MHD convective fluid flow for isothermal temperature, transport and concentration across a straight-up surface infinitely long enough with uniform boundary was found using the assumptions stated in this work and is expressed as follows:

The temperature, transport and concentration solution for isothermal condition from Eqs. (13) to (15)

$$u(y,t)=\left(1+\frac{b}{d}-\frac{b_1}{d_1}\right)G_1-\left(\frac{b}{d}\right)G-\left(\frac{b}{d}\right)R_4+\left(\frac{b}{d}\right)R+\left(\frac{b_1}{d_1}\right)I-\left(\frac{b_1}{d_1}\right)J+\left(\frac{b_1}{d_1}\right)J_1\tag{27}$$

$$\theta(y,t)=R_1(y,t)\tag{28}$$

$$C(y,t)=J_1(y,t)\tag{29}$$

where

$$F(y,t)=\left[e^{y\sqrt{\beta a^{*}}}\left(t\left(\frac{1}{2}\right)+\frac{y\sqrt{\beta}}{4\sqrt{a^{*}}}\right)erfc\left(\frac{y\sqrt{\beta}}{2\sqrt{t}}+\sqrt{ta^{*}}\right)\right]+\left[erfc\left(\frac{y\sqrt{\beta}}{2\sqrt{t}}-\sqrt{ta^{*}}\right)\left(t\left(\frac{1}{2}\right)-\frac{y\sqrt{\beta}}{4\sqrt{a^{*}}}\right)e^{-y\sqrt{\beta a^{*}}}\right]$$

$$F_1(y,t-1)=\left[e^{y\sqrt{a^{*}\beta}}\left((t-1)/2+\frac{y\sqrt{\beta}}{4\sqrt{a^{*}}}\right)erfc\left(\frac{y\sqrt{\beta}}{2\sqrt{-(1-t)}}+\sqrt{a^{*}t-a^{*}}\right)\right]+\left[e^{-y\sqrt{a^{*}\beta}}\left((t-1)/2-\frac{y\sqrt{\beta}}{4\sqrt{a^{*}}}\right)erfc\left(\frac{y\sqrt{\beta}}{2\sqrt{-(1-t)}}-\sqrt{a^{*}t-a^{*}}\right)\right]$$

$$G(y,t)=0.5e^{-dt}\left[e^{y\sqrt{\beta(a^{*}-d)}}\ erfc\left(\frac{y\sqrt{\beta}}{2\sqrt{t}}+\sqrt{(a^{*}-d)t}\right)+e^{-y\sqrt{\beta(a^{*}-d)}}\ erfc\left(\frac{y\sqrt{\beta}}{2\sqrt{t}}-\sqrt{(a^{*}-d)t}\right)\right]$$

$$G_1(y,t)=0.5\left[e^{-y\sqrt{\beta a^{*}}}erfc\left(\frac{y\sqrt{\beta}}{2\sqrt{t}}-\sqrt{ta^{*}}\right)+e^{y\sqrt{\beta a^{*}}}erfc\left(\frac{y\sqrt{\beta}}{2\sqrt{t}}+\sqrt{ta^{*}}\right)\right]$$

$$G_2(y,t-1)=0,5e^{-d(t-1)}\left[erfc\left(\frac{y\sqrt{\beta}}{2\sqrt{(t-1)}}+\sqrt{(a^{*}t-dt)-(a^{*}-d)}\right)e^{y\sqrt{\beta(a^{*}-d)}}+erfc\left(\frac{y\sqrt{\beta}}{2\sqrt{(t-1)}}-\sqrt{(a^{*}t-dt)-(a^{*}-d)}\right)e^{-y\sqrt{\beta(a^{*}-d)}}\right]$$

$$G_3(y,t-1)=0.5\left[erfc\left(\frac{y\sqrt{\beta}}{2\sqrt{-(1-t)}}+\sqrt{(a^{*}t-a^{*})}\right)e^{y\sqrt{\beta a^{*}}}+erfc\left(\frac{y\sqrt{\beta}}{2\sqrt{-(1-t)}}-\sqrt{(a^{*}t-a^{*})}\right)e^{-y\sqrt{\beta a^{*}}}\right]$$

$$I(y,t)=0,5e^{d_1t}\left[erfc\left(\frac{y\sqrt{\beta}}{2\sqrt{t}}+\sqrt{(a^{*}+d_1)t}\right)e^{y\sqrt{\beta(a^{*}+d_1)}}+erfc\left(\frac{y\sqrt{\beta}}{2\sqrt{t}}-\sqrt{(a^{*}+d_1)t}\right)e^{-y\sqrt{\beta(a^{*}+d_1)}}\right]$$

$$I_1(y,t)=0.5\left[erfc\left(\frac{y\sqrt{\beta}}{2\sqrt{t}}+\sqrt{\beta t}\right)e^{y\sqrt{\beta a^{*}}}+erfc\left(\frac{y\sqrt{\beta}}{2\sqrt{t}}-\sqrt{\beta t}\right)e^{-y\sqrt{\beta a^{*}}}\right]$$

$$I_2(y,t-1)=0.5e^{d_1(t-1)}\left[erfc\left(\frac{y\sqrt{\beta}}{2\sqrt{(t-1)}}+\sqrt{(a^{*}+d_1)(t-1)}\right)e^{y\sqrt{\beta(a^{*}+d_1)}}+erfc\left(\frac{y\sqrt{\beta}}{2\sqrt{(t-1)}}-\sqrt{(a^{*}+d_1)(t-1)}\right)e^{-y\sqrt{\beta(a^{*}+d_1)}}\right]$$

$$I_3(y,(t-1))=0.5\left[e^{y\sqrt{\beta a^{*}}}\ erfc\left(\frac{y\sqrt{\beta}}{2\sqrt{(t-1)}}+\sqrt{\beta t-\beta}\right)+e^{-y\sqrt{\beta a^{*}}}\ erfc\left(\frac{y\sqrt{\beta}}{2\sqrt{(t-1)}}-\sqrt{\beta t-\beta}\right)\right]$$

$$R(y,t)=0,5e^{-dt}\left[erfc\left(\frac{y\sqrt{\alpha}}{2\sqrt{t}}+\sqrt{(a_5-d)t}\right)e^{y\sqrt{\alpha(a_5-d)}}+erfc\left(\frac{y\sqrt{\alpha}}{2\sqrt{t}}-\sqrt{(a_5-d)t}\right)e^{-y\sqrt{\alpha(a_5-d)}}\right]$$

$$R_1(y,t)=0.5\left[erfc\left(\frac{y\sqrt{\alpha}}{2\sqrt{t}}+\sqrt{a_5t}\right)e^{(\sqrt{\alpha a_5})y}+erfc\left(\frac{y\sqrt{\alpha}}{2\sqrt{t}}-\sqrt{a_5t}\right)e^{-(\sqrt{\alpha a_5})y}\right]$$

$$\mathrm{R}_2(y,t)=\left[\left[\left(\frac{t}{2}+\frac{y\sqrt{\alpha}}{4\sqrt{a_5}}\right)e^{y\sqrt{\alpha a_5}}\ erfc\left(\frac{y\sqrt{\alpha}}{2\sqrt{t}}+\sqrt{a_5t}\right)\right]+\left[\left(\frac{t}{2}-\frac{y\sqrt{\alpha}}{4\sqrt{a_5}}\right)e^{-y\sqrt{\alpha a_5}}\ erfc\left(\frac{y\sqrt{\alpha}}{2\sqrt{t}}-\sqrt{a_5t}\right)\right]\right]$$

$$R_3(y,t-1)=0,5e^{-d(t-1)}\left[erfc\left(\frac{y\sqrt{\alpha}}{2\sqrt{-(1-t)}}+\sqrt{(t-1)(a_5-d)}\right)e^{\sqrt{\alpha(a_5-d)}y}+erfc\left(\frac{y\sqrt{\alpha}}{2\sqrt{-(1-t)}}-\sqrt{(t-1)(a_5-d)}\right)e^{-\sqrt{\alpha(a_5-d)}y}\right]$$

$$R_4(y,t-1)=0.5\left[erfc\left(\frac{y\sqrt{\alpha}}{2\sqrt{-(1-t)}}+\sqrt{a_5t-a_5}\right)e^{\sqrt{\alpha a_5}y}+erfc\left(\frac{y\sqrt{\alpha}}{2\sqrt{-(1-t)}}-\sqrt{a_5t-a_5}\right)e^{-\sqrt{\alpha a_5}y}\right]$$

$$\mathrm{R}_5(y,t-1)=\left[\left[\left((t-1)/2+\frac{y\sqrt{\alpha}}{4\sqrt{a_5}}\right)e^{y\sqrt{\alpha a_5}}\ erfc\left(\frac{y\sqrt{\alpha}}{2\sqrt{-(1-t)}}+\sqrt{a_5t-a_5}\right)\right]+\left[\left((t-1)/2-\frac{y\sqrt{\alpha}}{4\sqrt{a_5}}\right)e^{-y\sqrt{\alpha a_5}}\ erfc\left(\frac{y\sqrt{\alpha}}{2\sqrt{-(1-t)}}-\sqrt{a_5t-a_5}\right)\right]\right]$$

$$J(y,t)=0.5e^{d_1t}\left[e^{y\sqrt{d_1sc}}\ erfc\left(\frac{y\sqrt{sc}}{2\sqrt{t}}+\sqrt{d_1t}\right)+e^{-y\sqrt{d_1sc}}\ erfc\left(\frac{y\sqrt{sc}}{2\sqrt{t}}-\sqrt{d_1t}\right)\right]$$

$$J_1(y,t)=erfc\left(\frac{\sqrt{sc}}{2\sqrt{t}}y\right),\; J_2(y,t)=erfc\left(\frac{y\sqrt{sc}}{2\sqrt{t}}\right)\left(\frac{y^2\,sc}{2}+t\right)-ye^{-\left(\frac{y^2\,sc}{4t}\right)}\sqrt{\frac{t\,sc}{\pi}}$$

$$J_3(y,t-1)=\frac{e^{d_1(t-1)}}{2}\left[erfc\left(\frac{y\sqrt{sc}}{2\sqrt{(t-1)}}+\sqrt{d_1t-d_1}\right)e^{y\sqrt{d_1 sc}}+erfc\left(\frac{y\sqrt{sc}}{2\sqrt{(t-1)}}-\sqrt{d_1t-d_1}\right)e^{-y\sqrt{d_1 sc}}\right]$$

$$J_4(y,t-1)=erfc\left(\frac{\sqrt{sc}}{\sqrt{4(t-1)}}y\right)$$

4.1 Nusselt number

From the fluid temperature, heat flow rate can be computed from the non-dimensional form as

$$Nu=-\left(\frac{\partial\theta}{\partial y}\right)_{y=0} \tag{30}$$

Using Eq. (25), For Ramped wall temperature, we calculated the Nusselt number as follows:

$$Nu=-\left[N_1(t)+N_1(t-1)H(t-1)\right] \tag{31}$$

Using Eq. (28), for isothermal temperature, we calculated the Nusselt as follows:

$$Nu=-\left[N_2(t)\right] \tag{32}$$

where, $N_1(t)=-\dfrac{\sqrt{t\alpha}}{2\sqrt{\pi}}\left(e^{-a_5t}+e^{a_5t}\right)-t\sqrt{a_5\alpha}\;erf\left(\sqrt{a_5t}\right)-\dfrac{\sqrt{\alpha}}{2\sqrt{a_5}}erf\left(\sqrt{a_5\,t}\right)$

$$N_1(t-1)=-\left(e^{-a_5(t-1)}+e^{a_5(t-1)}\right)\left(\frac{\sqrt{(t-1)\alpha}}{2\sqrt{\pi}}\right)-(t-1)\sqrt{a_5\alpha}\;erf\left(\sqrt{a_5(t-1)}\right)-\frac{\sqrt{\alpha}}{2\sqrt{a_5}}erf\left(\sqrt{a_5(t-1)}\right)$$

$$N_2(t)=-\frac{\sqrt{\alpha}}{2\sqrt{\pi t}}\left(e^{-a_5t}+e^{a_5t}\right)-2\sqrt{\alpha a_5}\,erf\left(\sqrt{a_5t}\right)$$

4.2 Sherwood Number

From fluid concentration, mass flow rate computed from the non-dimensional form as

$$sh=-\left(\frac{\partial C}{\partial y}\right)_{y=0} \tag{33}$$

We derived the sherwood number for as follows using Eq. (26):

$$sh=\sqrt{4sc/\pi}\left[\sqrt{t}-H(t-1)\sqrt{(t-1)}\right] \tag{34}$$

where, $f(t)=-\frac{\sqrt{\beta t}}{2\sqrt{\pi}}(e^{-a^*t}+e^{a^*t})-t\sqrt{a^*\beta}\ erf(\sqrt{a^*t})-\frac{\sqrt{\beta}}{2\sqrt{a^*}}erf\ (\sqrt{a^*t})$

$$f_1(t-1)=-\frac{\sqrt{\beta(t-1)}}{2\sqrt{\pi}}(e^{-a^*(t-1)}+e^{a^*(t-1)})-\left(\sqrt{a^*\beta}\ erf\left(\sqrt{a^*t-a^*}\right)\right)(t-1)-\frac{\sqrt{\beta}}{2\sqrt{a^*}}erf\left(\sqrt{ta^*-a^*}\right)$$

$$g(t)=-\frac{\sqrt{\beta}}{\sqrt{\pi t}}(e^{-(a^*-d)t}+e^{(a^*-d)t})-2\sqrt{\beta(a^*-d)}\ erf\ (\sqrt{(a^*-d)t})$$

$$g_1(t)=-\frac{\sqrt{\beta}}{\sqrt{\pi t}}(e^{-a^*t}+e^{a^*t})-2\sqrt{\beta a^*}\ erf\ (\sqrt{a^*t})$$

$$g_2(t-1)=-\sqrt{\beta(t-1)\pi}\,(e^{-(a^*-d)(t-1)}+e^{(a^*-d)(t-1)})-2\sqrt{\beta(a^*-d)}\ erf\ (\sqrt{(a^*-d)(t-1)})$$

$$g_3(t-1)=-\sqrt{\beta/(t-1)\pi}\,(e^{-(a^*t-a^*)}+e^{(a^*t-a^*)})-2\sqrt{a^*\beta}\ erf\ (\sqrt{(t-1)a^*})$$

$$i(t)=-\sqrt{\beta/\pi t}\,(e^{-(a^*+d_1)t}+e^{(a^*+d_1)t})-2\sqrt{\beta(a^*+d_1)}\ erf\ (\sqrt{(a^*+d_1)t})$$

$$i_1(t)=\sqrt{\beta/\pi t}\,(e^{-a^*t}+e^{a^*t})-2\sqrt{\beta a^*}\ erf\ (\sqrt{a^*t})$$

$$i_2(t-1)=-\sqrt{\beta/\pi(t-1)}\,(e^{-(a^*+d_1)(t-1)}+e^{(a^*+d_1)(t-1)})-2\sqrt{\beta(a^*+d_1)}\ erf\ (\sqrt{(a^*+d_1)(t-1)})$$

$$i_3(t-1)=-\sqrt{\beta/\pi(t-1)}(e^{-(a^*t-a^*)}+e^{(a^*t-a^*)})-2\sqrt{a^*\beta}\ erf\ (\sqrt{(t-1)a^*})$$

$$r(t)=-\sqrt{\alpha/\pi t}\,(e^{-(a_5-d)t}+e^{(a_5-d)t})-2\sqrt{\alpha(a_5-d)}\ erf\ (\sqrt{(a_5-d)t})$$

$$r_1(t)=-\sqrt{\alpha/\pi t}\,(e^{-a_5t}+e^{a_5t})-2\sqrt{\alpha a_5}\ erf\ (\sqrt{a_5t})$$

$$r_2(t)=-\sqrt{\alpha t/4\pi}(e^{-a_5t}+e^{a_5t})-t\sqrt{a_5\alpha}\ erf(\sqrt{a_5t})-\frac{\sqrt{\alpha}}{2\sqrt{a_5}}erf\ (\sqrt{a_5t})$$

$$r_3(t-1)=-\frac{\sqrt{\alpha}}{\sqrt{\pi t-\pi}}(e^{-(a_5-d)(t-1)}+e^{(a_5-d)(t-1)})-2\sqrt{\alpha(a_5-d)}\ erf\ (\sqrt{(a_5-d)(t-1)})$$

$$r_4(t-1)=-\frac{\sqrt{\alpha}}{\sqrt{\pi t-\pi}}(e^{-(a_5t-a_5)}+e^{(a_5t-a_5)})-2\sqrt{a_5\alpha}\ erf\ (\sqrt{(t-1)a_5})$$

$$r5(t-1)=-\sqrt{\alpha(t-1)/(4\pi)}(e^{-a_5(t-1)}+e^{a_5(t-1)})-(t-1)\sqrt{a_5\alpha}\ erf(\sqrt{a_5(t-1)})-\frac{\sqrt{\alpha}}{2\sqrt{a_5}}erf\ (\sqrt{a_5(t-1)})$$

$$j(t)=-\sqrt{\frac{sc}{\pi t}}\left(e^{-d_1t}+e^{d_1t}\right)-2\sqrt{d_1\,sc}\,erf\left(\sqrt{d_1t}\right)$$

$$j_1(t)=-\sqrt{\frac{sc}{\pi t}}$$

$$j_2(t)=-2\sqrt{\frac{t\,sc}{\pi}}$$

$$j_3(t-1)=-\sqrt{\frac{sc}{(t-1)\pi}}\left(e^{-(d_1t-d_1)}+e^{(d_1t-d_1)}\right)-2\sqrt{scd_1}\ erf\left(\sqrt{(t-1)d_1}\right)$$

$$j_4(t)=-\sqrt{\frac{sc}{\pi(t-1)}},\ j_5(t-1)=-\sqrt{4(t-1)\,sc/\pi}$$

$$J_5(y,t-1)=\left(\frac{y^2\,sc}{2}+(t-1)\right)erfc\left(\frac{y\sqrt{sc}}{2\sqrt{(t-1)}}\right)-y\sqrt{\frac{(t-1)\,sc}{\pi}}\,e^{-\frac{y^2\,sc}{4(t-1)}}$$

5. Parametric Study

To understand the physical mechanism of present problems, a parametric analysis has been accomplished. We have calculated solutions for the said problems and the values are represented in graphs and tables below. For both ramped $(0 < t \leq 1)$ and isothermal $(t \geq 1)$wall boundaries, the physical characteristics of related quantities appearing in the solution model are studied and plotted graphs on flow transport, fluid temperature and species mass besides that tables including numerical simulations are used to explain the role of related parameters in determining heat and mass transmission. Nanoparticles and base fluid physical parameters are listed in Table 1. The Ramping case was depicted by solid lines, whereas the Isothermal case was represented by dotted lines.

Table 1
Thermophoresis properties of water and nanoparticles [58]

Thermo-physical properties	Gasoline	Al_2O_3
$\rho(kg/m)$	751	3970
$C_p(J/kgK)$	2.06	765
$k(w/mK)$	0.1164	46
$\beta \times 10^5 (K^{-1})$	8.591	0.0217
ϕ	0.00	0.2

The influence of the radiation parameter, as shown in Figure 2, demonstrates with increasing Nr, fluid temperature increases with both ramping and isothermal conditions for both boron and aluminium oxide nanoparticles. In both circumstances, thermal radiation improves the fluid temperature throughout the boundary area. It's stable because, this thermal radiation adds to diffuse energy since the thermal radiation parameter. Figure 3 depict the effect of φ (Nano-sized particle volume fraction) on fluid temperature, hence noticed that with increasing φ of the nanoparticle decreases the temperature profile for both Ramped and isothermal condition as well as for both nanoparticles.

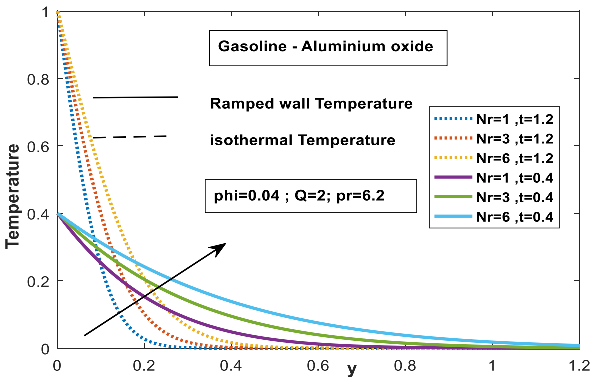

Fig. 2. Various values of Nr for temperature

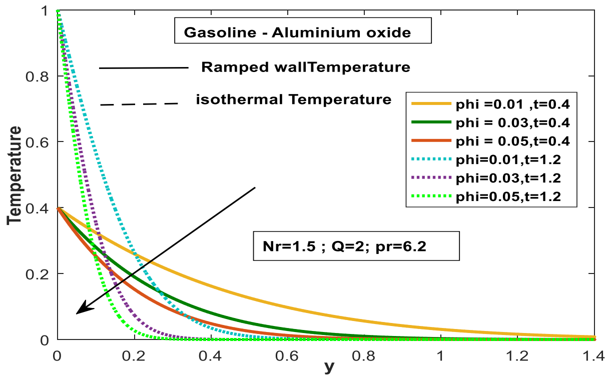

Fig. 3. Various values of volume fraction for temperature

The temperature profiles for various values of Prandtl number are highlighted in Figure 4. The impact of Pr on the distribution of temperature field in a case of ramped temperature as well as isothermal plates. It is noted that the nanofluid temperature diminishes as a result of enlarging Pr values in the case of isothermal. The essence of this decline is that fluids thermal conductivity is weakened by an upturn in Pr values, reducing heat transfer and therefore temperature. And then

Prandtl boundary layer width minimizes. But in ramped temperature, the temperature increased with increases of Prandtl number. The dual character of the flow profile is due to the nonuniform impact of time variables on the thermal boundary layer. The value of t=0.4 for ramped conditions and for isothermal condition t=1.2.

Figures 5 show the impact of heat source/sink on the temperature of the nanofluids. Notably, temperature decrease with increasing of heat source parameter. As the heat source parameter increases, more heat is absorbed, implying that the hotness of the fluid reduces with the higher magnitude of Q. Heat transmission may be successfully managed by adding a heat sink to the system.

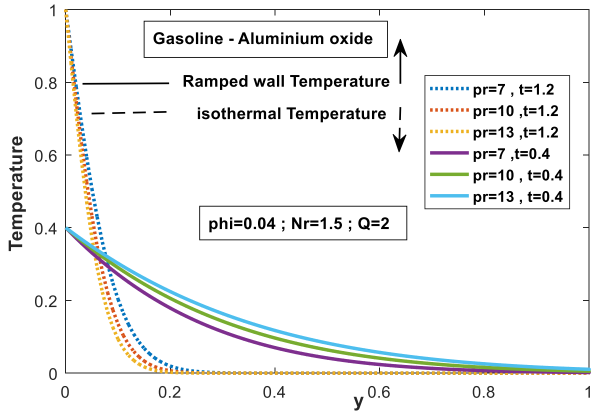

Fig. 4. Various values of Pr for temperature

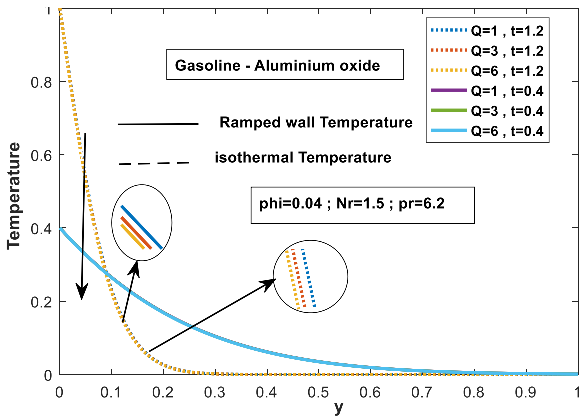

Fig. 5. Various values of heat source for temperature

Figures 6 illustrate how temperature grew as time t increased. Near the plate, the nanofluid's temperature is highest, and it gradually decreases until it reaches a point where it is no longer hotter than the free stream. For different magnitudes sc and t, the curve patterns on the species are represented in Figures 7-8. It has been noticed that in the ramped case also in constant species of mass, the concentration drops as a raise in Schmidt number, but increases as t increases.

The velocity profiles for different values of k are shown in Figure 9 while the other parameters are held constant. Increasing the value of k causes the thickness of the momentum boundary layer to rise, according to the graph. The physical explanation for this is that increasing k lowers the resistance given by a porous medium, which improves the momentum development of the regime and, as a result, increases the fluid's velocity.

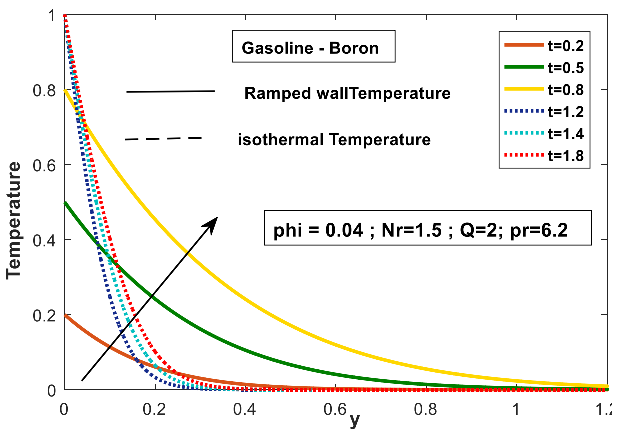

Fig. 6. Various values of t for temperature

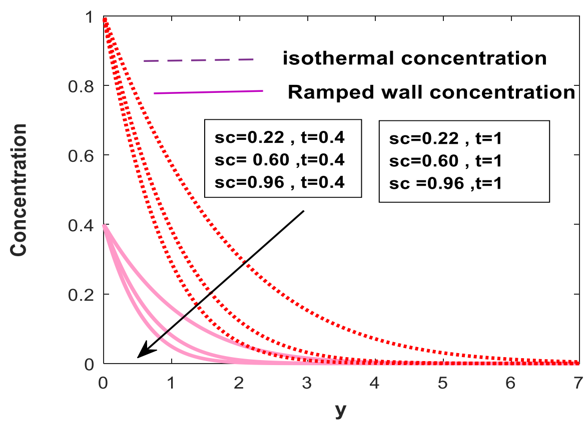

Fig. 7. Various values of sc for concentration

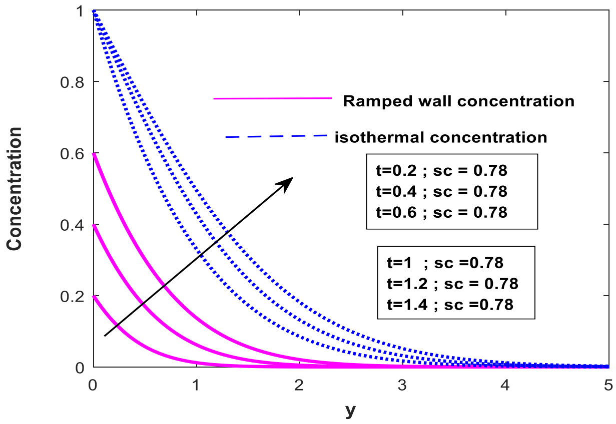

Fig. 8. Various values of t for concentration

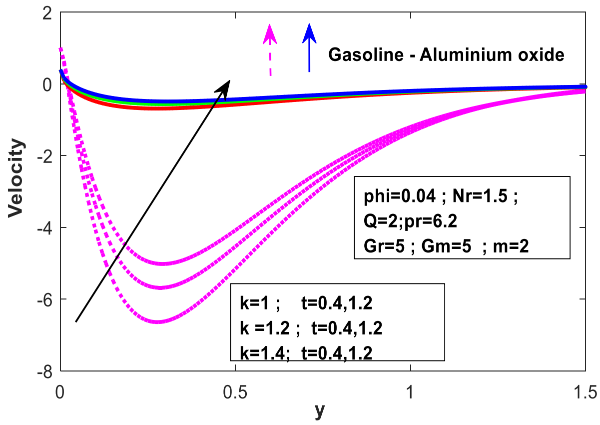

Fig. 9. Various values of porosity for velocity

Magnetic parameter (M) has an impact on velocity distribution in ramping and isothermal conditions, as seen in Figure 10. Nanofluid velocity has been demonstrated to have a negative effect on the function of M. Magnetic lines, also known as the Lorentz force, derived from Ohm's law and one of Maxwell's equations, may have a greater impact on the velocity boundary near the plate and induce slowdowns as a result of this influence. Lorentz force is produced once a magnetic field is applied to an electrified insulated nanofluid, which acts as a dragging force. When M is increased, the Lorentz force becomes more powerful, allowing the nanofluid to slowly come to a stop.

Figure 11 illustrates the influence of the volume fraction of nanoparticle ϕ on dimensionless velocity. In both ramping and isothermal conditions, the velocity of nanofluids is increased. But in general, adding nanoparticles to a fluid increases its density, which reduces both the boundary layer thickness as well as nanofluid velocity.

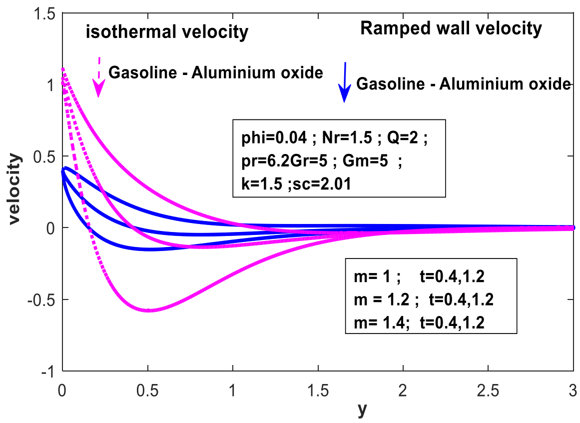

Fig. 10. Various values of magnetic field for velocity

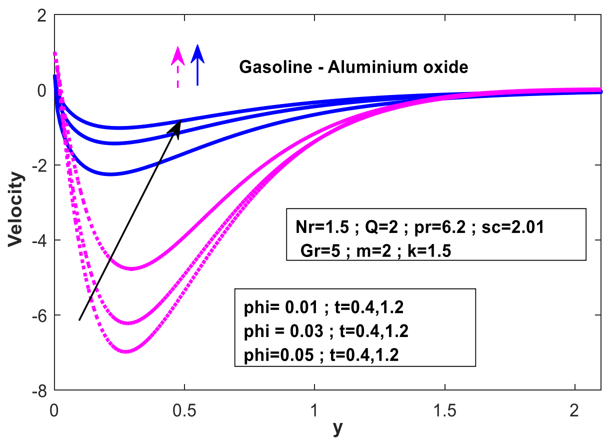

Fig. 11. Various values of porosity for velocity

Isothermal and ramping conditions, as well as the impacts of altering parameters, are depicted in Figures 12-16, some interesting facts noted down for variance parameters, the velocity function exhibits two distinct behaviours. The non-uniform impact of t on the momentum boundary layer thickness accounts for the dual character of the flow profile. For ramping conditions, t = 0.4, and for isothermal conditions, t = 1.2.

More exactly, Nr and Gr increase the velocity of nanofluid under isothermal conditions and reduce the velocity function under ramping conditions. The major cause of the velocity function's

Journal of Research in Nanoscience and Nanotechnology
Volume 15, Issue 1 (2025) 1-22

opposing behaviour is the non-uniform influence of time t on the boundary layer thickness of momentum. The rate of t=1.2 under isothermal conditions, which is the reason of momentum boundary layer expands as the rate of Nr and Gr hike, further it decreases under the impact of ramping for increasing variation of Nr and Gr since the time value for this condition is fairly small (t=0.4). Figures 14-16 show the same explanation for the inverse effects: when the values of Q, pr, and Gm rise, the velocity for the ramped condition increases, while the velocity for the isothermal state falls due to time influence. The velocity profiles for various Schmidt numbers (Sc) are illustrated in Figure 17, and the velocity rises with higher Schmidt numbers. Schmidt number = kinematic viscosity / momentum diffusivity.

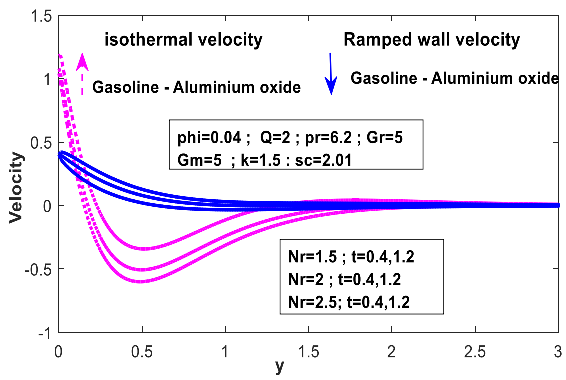

Fig. 12. Various values of Nr for velocity

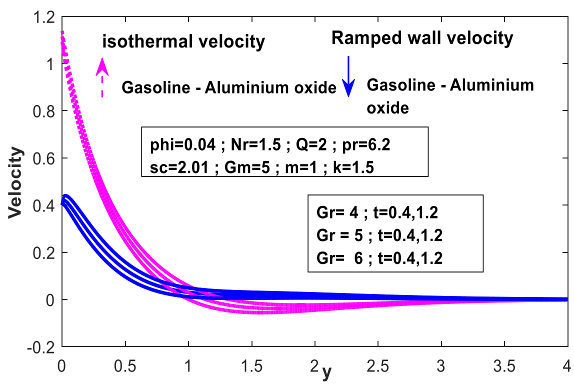

Fig. 13. Various values of Gr for velocity

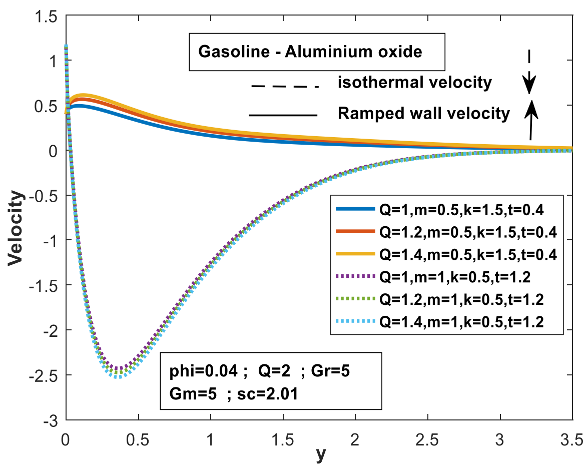

Fig. 14. Various values of heat source for velocity

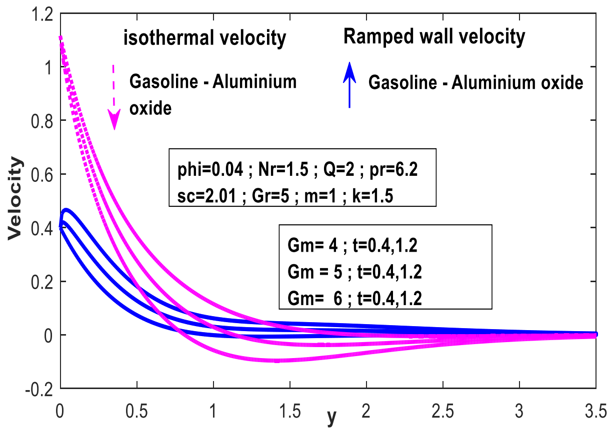

Fig. 15. Various values of Gm for velocity

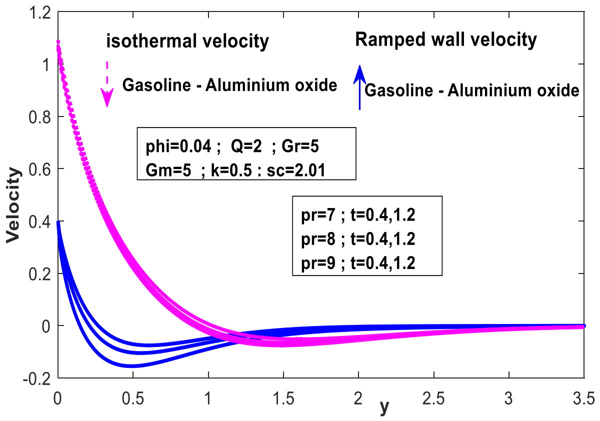

Fig. 16. Various values of Pr for velocity

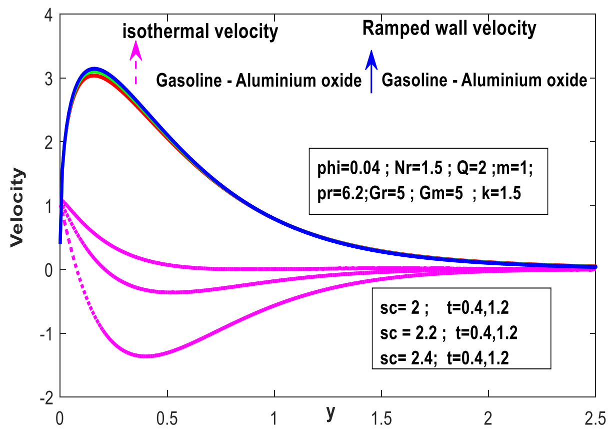

Fig. 17. Various values of sc for velocity

The non-dimensional mass flow rate, heat flow rate and shear stress rate for both (Al_2O_3-H_2O and B-H_2O) nanofluids for different values of several parameters are determined which was mentioned in Table 2 to Table 3. For both ramping and isothermal wall temperatures, the Sherwood number Sh rises in magnitudely with increasing t (Table 2). The Nusselt number Nu drops as pr, Nr, grows for both ramping and isothermal situations, whereas Nu increases when ϕ ,Q increases (Table 3).

Table 2
The Sherwood number variation

Sc	t		Shearwood number for isothermal temperature	Shearwood number for Ramped wall temperature
0.22	1.2	0.2	-0.3430809026	-0.2366908109
0.60	1.2	0.2	-0.5665794634	-0.3908820095
0.78	1.4		-0.5488644301	
0.78	1.6		-0.4886264860	
0.78		0.4		-0.6302783019
0.78		0.6		-0.7719301179

Table 3
Nusselt number variation

ϕ	Pr	t		Q	Nr	Nusselt number for isothermal temperature	Nusselt number for ramped wall temperature
						Aluminium Oxide (Al2O3)	Aluminium Oxide (Al2O3)
0.01	6.2	1	0.2	2	1.5	0.972278976185802	0.340781511246800
0.02	6.2	1	0.2	2	1.5	1.187241493920871	0.449726196194241
0.03	6.2	1	0.2	2	1.5	1.360419306081635	0.533279605411406
	7.0	1	0.2	2	1.5	1.280323188430491	0.501882207693629
	8.0	1	0.2	2	1.5	1.197632678862229	0.469467817426820
		1.2	0.3	2	1.5	0.874704446391998	0.588126469715958
		1.4	0.4	2	1.5	0.792526868794893	0.692540897092866
			0.5	2	1.5	0.792526868794893	0.788047937296101
				2.2	1.5	0.809946420435267	0.794579969376230
				2.4	1.5	0.826972053814545	0.800920757393285
					1.7	0.796803058413768	0.771702146516740
					1.9	0.769711938960168	0.745464452254491

6. Conclusion

Present investigation PDEs with ramping wall boundary conditions of a nanofluid flow, suspended boron and aluminium oxide nanoparticles in the base fluid, driven by magnetic and gravitational forces in a semi-infinite flow area was solved using the integral transform approach. In the momentum equation, Bousinessq's approximation is used to simplify the pressure gradient and body force, whereas, in the energy equation, temperature-dependent heat absorption and optically thick heat radiating are used. Heavyside, exponential, and complementary error functions were used to address fluid temperature, transport, and species concentration.

Noteworthy results are summarized below:

i) The velocity profile for both nanofluids are reduced as increasing magnetic field parameter
ii) For both nanofluids the velocity profiles are increased as an increase of porosity medium
iii) The momentum boundary layer and concentration boundary layer reduce as an increase in nanoparticles volume fraction, but the energy boundary layer is increased for both the nanofluids
iv) In both ramped and isothermal conditions, the temperature profiles increase with increasing the values of heat absorption/ generation parameter for both the nanofluids. But in the velocity profile its increases in isothermal, whereas it is noticed that the opposite reaction in ramped condition due to the time nature.
v) Temperature increases with increasing of time t
vi) Concentration decreases with an increase in Schmidt number Sc while increases with the progress of time.

References

1. Choi, S. US, and Jeffrey A. Eastman. *Enhancing thermal conductivity of fluids with nanoparticles*. No. ANL/MSD/CP-84938; CONF-951135-29. Argonne National Lab.(ANL), Argonne, IL (United States), 1995
2. Daniel Makinde, Oluwole. "Computational modelling of nanofluids flow over a convectively heated unsteady stretching sheet." *Current Nanoscience* 9, no. 5 (2013): 673-678. https://doi.org/10.2174/15734137113099990068
3. Eastman, Jeffery A., U. S. Choi, Shaoping Li, L. J. Thompson, and Shinpyo Lee. "Enhanced thermal conductivity through the development of nanofluids." *MRS Online Proceedings Library (OPL)* 457 (1996): 3. https://doi.org/10.1557/PROC-457-3
4. Eastman, Jeffrey A., S. U. S. Choi, Sheng Li, W. Yu, and L. J. Thompson. "Anomalously increased effective thermal conductivities of ethylene glycol-based nanofluids containing copper nanoparticles." *Applied physics letters* 78, no. 6 (2001): 718-720. https://doi.org/10.1063/1.1341218
5. Elfaghi, Abdulhafid MA, Alhadi A. Abosbaia, Munir FA Alkbir, and Abdoulhdi AB Omran. "CFD simulation of forced convection heat transfer enhancement in pipe using Al2O3/water nanofluid." *Journal of Advanced Research in Numerical Heat Transfer* 8, no. 1 (2022): 44-49. https://doi.org/10.37934/cfdl.14.9.118124
6. Muhammad, Nura Muaz, Nor Azwadi Che Sidik, Aminuddin Saat, Yusuf Alhassan, and Yutaka Asako. "A Numerical Investigation on the Combined Effect of Aluminum-Nitride/Water Nanofluid with Different Mini-Scale Geometries for Passive Hydrothermal Augmentation." *Journal of Advanced Research in Numerical Heat Transfer* 1, no. 1 (2020): 1-12.
7. Makinde, O. D., W. A. Khan, and Z. H. Khan. "Buoyancy effects on MHD stagnation point flow and heat transfer of a nanofluid past a convectively heated stretching/shrinking sheet." *International journal of heat and mass transfer* 62 (2013): 526-533. https://doi.org/10.1016/j.ijheatmasstransfer.2013.03.049

8. Chamkha, Ali J., and A. M. Aly. "MHD free convection flow of a nanofluid past a vertical plate in the presence of heat generation or absorption effects." *Chemical Engineering Communications* 198, no. 3 (2010): 425-441. https://doi.org/10.1080/00986445.2010.520232
9. Nayak, M. K., Noreen Sher Akbar, V. S. Pandey, Zafar Hayat Khan, and Dharmendra Tripathi. "3D free convective MHD flow of nanofluid over permeable linear stretching sheet with thermal radiation." *Powder Technology* 315 (2017): 205-215. https://doi.org/10.1016/j.powtec.2017.04.017
10. Turkyilmazoglu, M., and I. Pop. "Heat and mass transfer of unsteady natural convection flow of some nanofluids past a vertical infinite flat plate with radiation effect." *International Journal of Heat and Mass Transfer* 59 (2013): 167-171. https://doi.org/10.1016/j.ijheatmasstransfer.2012.12.009
11. Sheikholeslami, Mohsen, Davood Domiri Ganji, M. Younus Javed, and R. Ellahi. "Effect of thermal radiation on magnetohydrodynamics nanofluid flow and heat transfer by means of two phase model." *Journal of magnetism and Magnetic materials* 374 (2015): 36-43. https://doi.org/10.1016/j.jmmm.2014.08.021
12. Chamkha, Ali J. "Hydromagnetic natural convection from an isothermal inclined surface adjacent to a thermally stratified porous medium." *International Journal of Engineering Science* 35, no. 10-11 (1997): 975-986. https://doi.org/10.1016/S0020-7225(96)00122-X
13. Chamkha, Ali J. "Thermal radiation and buoyancy effects on hydromagnetic flow over an accelerating permeable surface with heat source or sink." *International Journal of Engineering Science* 38, no. 15 (2000): 1699-1712. https://doi.org/10.1016/S0020-7225(99)00134-2
14. Krishna, M. Veera, N. Ameer Ahamad, and Ali J. Chamkha. "Radiation absorption on MHD convective flow of nanofluids through vertically travelling absorbent plate." *Ain Shams Engineering Journal* 12, no. 3 (2021): 3043-3056. https://doi.org/10.1016/j.asej.2020.10.028
15. Prakash, Jagdish, D. Bhanumathi, A. G. Vijaya Kumar, and S. V. K. Varma. "Diffusion-thermo and radiation effects on unsteady MHD flow through porous medium past an impulsively started infinite vertical plate with variable temperature and mass diffusion." *Transport in Porous Media* 96, no. 1 (2013): 135-151. https://doi.org/10.1007/s11242-012-0078-x
16. Ewis, Karem Mahmoud. "Effects of Variable Thermal Conductivity and Grashof Number on Non-Darcian Natural Convection Flow of Viscoelastic Fluids with Non Linear Radiation and Dissipations." *Journal of Advanced Research in Applied Sciences and Engineering Technology* 22, no. 1 (2021): 69-80. https://doi.org/10.37934/araset.22.1.6980
17. Teh, Yuan Ying, and Adnan Ashgar. "Three dimensional MHD hybrid nanofluid Flow with rotating stretching/shrinking sheet and Joule heating." *CFD Letters* 13, no. 8 (2021): 1-19. https://doi.org/10.37934/cfdl.13.8.119
18. Adnan, Nurul Shahirah Mohd, Ahmad Nazri Mohamad Som, Norihan Md Arifin, Norfifah Bachok, Fadzilah Md Ali, and Yong Faezah Rahim. "A stability analysis of boundary layer stagnation-point slip flow and heat transfer towards a shrinking/stretching cylinder over a permeable surface." *CFD Letters* 12, no. 11 (2020): 97-105. https://doi.org/10.37934/cfdl.12.11.97105
19. Azman, Azraf, Mohd Zamri Yusoff, Azfarizal Mukhtar, Prem Gunnasegaran, Nasri A. Hamid, and Ng Khai Ching. "Numerical study of heat transfer enhancement for mono and hybrid nanofluids flow in a straight pipe." *CFD Letters* 13, no. 2 (2021): 49-61. https://doi.org/10.37934/cfdl.13.2.4961
20. Ferdows, Mohammad, Mohammed Shamshuddin, and Khairy Zaimi. "Computation of steady free convective boundary layer viscous fluid flow and heat transfer towards the moving flat subjected to suction/injection effects." *CFD Letters* 13, no. 3 (2021): 16-24. https://doi.org/10.37934/cfdl.13.3.1624
21. Sharafatmandjoor, Shervin. "Effects of the optimal imposition of viscous and thermal forces on spectral dynamical features of swimming of a microorganism in nanofluids." *Journal of Advanced Research in Micro and Nano Engineering* 8, no. 1 (2022): 1-8.
22. Ahmed, Waqar, Nor Azwadi Che Sidik, and Yutaka Asako. "Metal oxide and ethylene glycol based well stable nanofluids for mass flow in closed conduit." *Journal of Advanced Research in Micro and Nano Engineering* 6, no. 1 (2021): 1-15.

23. Hamad, M. A. A., I. Pop, and AI Md Ismail. "Magnetic field effects on free convection flow of a nanofluid past a vertical semi-infinite flat plate." *Nonlinear Analysis: Real World Applications* 12, no. 3 (2011): 1338-1346. https://doi.org/10.1016/j.nonrwa.2010.09.014
24. Das, S., and R. N. Jana. "Natural convective magneto-nanofluid flow and radiative heat transfer past a moving vertical plate." *Alexandria Engineering Journal* 54, no. 1 (2015): 55-64. https://doi.org/10.1016/j.aej.2015.01.001
25. Hussanan, Abid, Ilyas Khan, Hasmawani Hashim, Muhammad Khairul Anuar, Nazila Ishak, Norhafizah Md Sarif, and Mohd Zuki Salleh. "Unsteady MHD flow of some nanofluids past an accelerated vertical plate embedded in a porous medium." *Jurnal Teknologi (Sciences & Engineering)* 78, no. 2 (2016). https://doi.org/10.11113/jt.v78.4900
26. Sheikholeslami, M., T. Hayat, and AJIJoH Alsaedi. "MHD free convection of Al2O3–water nanofluid considering thermal radiation: a numerical study." *International Journal of Heat and Mass Transfer* 96 (2016): 513-524. https://doi.org/10.1016/j.ijheatmasstransfer.2016.01.059
27. Das, S., R. N. Jana, and O. D. Makinde. "MHD boundary layer slip flow and heat transfer of nanofluid past a vertical stretching sheet with non-uniform heat generation/absorption." *International Journal of Nanoscience* 13, no. 03 (2014): 1450019. https://doi.org/10.1142/S0219581X14500197
28. Chamkha, Ali J., and A. M. Aly. "MHD free convection flow of a nanofluid past a vertical plate in the presence of heat generation or absorption effects." *Chemical Engineering Communications* 198, no. 3 (2010): 425-441. https://doi.org/10.1080/00986445.2010.520232
29. Soomro, Feroz Ahmed, Rizwan Ul Haq, Qasem M. Al-Mdallal, and Qiang Zhang. "Heat generation/absorption and nonlinear radiation effects on stagnation point flow of nanofluid along a moving surface." *Results in physics* 8 (2018): 404-414. https://doi.org/10.1016/j.rinp.2017.12.037
30. Hayat, Tasawar, Muhammad Ijaz Khan, Muhammad Waqas, and Ahmed Alsaedi. "On the performance of heat absorption/generation and thermal stratification in mixed convective flow of an Oldroyd-B fluid." *Nuclear Engineering and Technology* 49, no. 8 (2017): 1645-1653. https://doi.org/10.1016/j.net.2017.07.027
31. Khan, Arshad, Dolat Khan, Ilyas Khan, Farhad Ali, and Muhammad Imran. "MHD flow of sodium alginate-based Casson type nanofluid passing through a porous medium with Newtonian heating." *Scientific reports* 8, no. 1 (2018): 1-12. https://doi.org/10.1038/s41598-018-26994-1
32. Kumaresan, E., AG Vijaya Kumar, and B. Rushi Kumar. "Chemically reacting on MHD boundary layer flow of CuO-water and MgO-water nanofluids past a stretching sheet in porous media with radiation absorption and heat generation/absorption." In *IOP Conference Series: Materials Science and Engineering*, vol. 263, no. 6, p. 062017. IOP Publishing, 2017. https://doi.org/10.1088/1757-899X/263/6/062017
33. Mahat, Rahimah, Sharidan Shafie, and Fatihhi Januddi. "Numerical analysis of mixed convection flow past a symmetric cylinder with viscous dissipation in viscoelastic nanofluid." *CFD letters* 13, no. 2 (2021): 12-28. https://doi.org/10.37934/cfdl.13.2.1228
34. Jowsey, Mohamad Hafzan Mohamad, Natrah Kamaruzaman, and Mohsin Mohd Sies. "Heat and flow profile of nanofluid flow inside multilayer microchannel heat sink." *Journal of Advanced Research in Micro and Nano Engineering* 4, no. 1 (2021): 1-9.
35. Akaje, Wasiu, and B. I. Olajuwon. "Impacts of Nonlinear thermal radiation on a stagnation point of an aligned MHD Casson nanofluid flow with Thompson and Troian slip boundary condition." *Journal of Advanced Research in Experimental Fluid Mechanics and Heat Transfer* 6, no. 1 (2021): 1-15.
36. Sidik, Nor Azwadi Che, Saidu Bello Abubakar, and Siti Nurul Akmal Yusof. "Measurement of Fluid Flow and Heat Transfer Performance in Rectangular Microchannel using Pure Water and Fe3O4-H2O Nanofluid." *Journal of Advanced Research in Applied Mechanics* 68, no. 1 (2020): 9-21. https://doi.org/10.37934/aram.68.1.921
37. Sidik, Nor Azwadi Che, Abdolbaqi Mohammed Khdher, Siti Nurul Akmal Yusof, and M'hamed Beriache. "Heat Transfer Enhancement in Straight Channel with Nanofluid In Fully Developed Turbulent Flow." *Journal of Advanced Research in Applied Mechanics* 63, no. 1 (2019): 1-15.

38. Sheri, Siva Reddy, Ali J. Chamkha, and Anjan Kumar Suram. "Heat and mass transfer effects on MHD natural convection flow past an impulsively moving vertical plate with ramped temperature." *American Journal of heat and mass transfer* 3, no. 3 (2016): 129-148. https://doi.org/10.7726/ajhmt.2016.1009
39. Seth, G. S., R. Sharma, and S. Sarkar. "Natural convection heat and mass transfer flow with Hall current, rotation, radiation and heat absorption past an accelerated moving vertical plate with ramped temperature." *Journal of Applied Fluid Mechanics* 8, no. 1 (2014): 7-20. https://doi.org/10.36884/jafm.8.01.22600
40. Seth, G. S., B. Kumbhakar, and R. Sharma. "Unsteady MHD free convection flow with Hall effect of a radiating and heat absorbing fluid past a moving vertical plate with variable ramped temperature." *Journal of the Egyptian Mathematical Society* 24, no. 3 (2016): 471-478. https://doi.org/10.1016/j.joems.2015.07.007
41. Ahmed, N., and M. Dutta. "Transient mass transfer flow past an impulsively started infinite vertical plate with ramped plate velocity and ramped temperature." *Int. J. Phys. Sci* 8, no. 7 (2013): 254-263.
42. Chandran, Pallath, Nirmal C. Sacheti, and Ashok K. Singh. "Natural convection near a vertical plate with ramped wall temperature." *Heat and Mass Transfer* 41 (2005): 459-464. https://doi.org/10.1007/s00231-004-0568-7
43. Kataria, Hari R., and Harshad R. Patel. "Effect of thermo-diffusion and parabolic motion on MHD Second grade fluid flow with ramped wall temperature and ramped surface concentration." *Alexandria Engineering Journal* 57, no. 1 (2018): 73-85. https://doi.org/10.1016/j.aej.2016.11.014
44. Sheri, Siva Reddy, R. Srinivasa Raju, and S. Anjan Kumar. "Transient approach to heat absorption and radiative heat transfer past an impulsively moving plate with ramped temperature." *Procedia Engineering* 127 (2015): 893-900. https://doi.org/10.1016/j.proeng.2015.11.427
45. Seth, G. S., Md S. Ansari, and R. Nandkeolyar. "MHD natural convection flow with radiative heat transfer past an impulsively moving plate with ramped wall temperature." *Heat and mass transfer* 47 (2011): 551-561. https://doi.org/10.1007/s00231-010-0740-1
46. Narahari, Marneni, Osman Anwar Bég, and Swapan Kumar Ghosh. "Mathematical modelling of mass transfer and free convection current effects on unsteady viscous flow with ramped wall temperature." (2011). https://doi.org/10.4236/wjm.2011.14023
47. Seth, G. S., and S. Sarkar. "MHD natural convection heat and mass transfer flow past a time dependent moving vertical plate with ramped temperature in a rotating medium with Hall effects, radiation and chemical reaction." *Journal of Mechanics* 31, no. 1 (2015): 91-104. https://doi.org/10.1017/jmech.2014.71
48. Seth, G. S., S. Sarkar, S. M. Hussain, and G. K. Mahato. "Effects of hall current and rotation on hydromagnetic natural convection flow with heat and mass transfer of a heat absorbing fluid past an impulsively moving vertical plate with ramped temperature." *Journal of Applied Fluid Mechanics* 8, no. 1 (2014): 159-171. https://doi.org/10.36884/jafm.8.01.20437
49. VeeraKrishna, M., and Ali J. Chamkha. "Hall effects on unsteady MHD flow of second grade fluid through porous medium with ramped wall temperature and ramped surface concentration." *Physics of Fluids* 30, no. 5 (2018). https://doi.org/10.1063/1.5025542
50. Kataria, Hari R., and Harshad R. Patel. "Effects of chemical reaction and heat generation/absorption on magnetohydrodynamic (MHD) Casson fluid flow over an exponentially accelerated vertical plate embedded in porous medium with ramped wall temperature and ramped surface concentration." *Propulsion and Power Research* 8, no. 1 (2019): 35-46. https://doi.org/10.1016/j.jppr.2018.12.001
51. Anwar, Talha, Poom Kumam, and Wiboonsak Watthayu. "Unsteady MHD natural convection flow of Casson fluid incorporating thermal radiative flux and heat injection/suction mechanism under variable wall conditions." *Scientific reports* 11, no. 1 (2021): 4275. https://doi.org/10.1038/s41598-021-83691-2
52. Kataria, Hari R., and Akhil S. Mittal. "Velocity, mass and temperature analysis of gravity-driven convection nanofluid flow past an oscillating vertical plate in the presence of magnetic field in a porous medium." *Applied Thermal Engineering* 110 (2017): 864-874. https://doi.org/10.1016/j.applthermaleng.2016.08.129

53. VeeraKrishna, M., and Ali J. Chamkha. "Hall effects on unsteady MHD flow of second grade fluid through porous medium with ramped wall temperature and ramped surface concentration." *Physics of Fluids* 30, no. 5 (2018). https://doi.org/10.1063/1.5025542
54. Khan, Ansab Azam, Khairy Zaimi, Suliadi Firdaus Sufahani, and Mohammad Ferdows. "MHD flow and heat transfer of double stratified micropolar fluid over a vertical permeable shrinking/stretching sheet with chemical reaction and heat source." *Journal of Advanced Research in Applied Sciences and Engineering Technology* 21, no. 1 (2020): 1-14. https://doi.org/10.37934/araset.21.1.114
55. Pasha, Amjad Ali, Meshal Nuwaym Al-Harbi, Surfarazhussain S. Halkarni, Nazrul Islam, D. Siva Krishna Reddy, S. Nadaraja Pillai, and Ufaith Qadiri. "CFD study of Convective Heat Transfer of Water Flow Through Micro-Pipe with Mixed Constant Wall Temperature and Heat Flux Wall Boundary Conditions." *CFD Letters* 13, no. 7 (2021): 13-26. https://doi.org/10.37934/cfdl.13.7.1326
56. Zokri, Syazwani Mohd, Nur Syamilah Arifin, Abdul Rahman Mohd Kasim, and Mohd Zuki Salleh. "Free convection boundary layer flow of Jeffrey nanofluid on a horizontal circular cylinder with viscous dissipation effect." *Journal of Advanced Research in Micro and Nano Engineering* 1, no. 1 (2020): 1-14. https://doi.org/10.37934/cfdl.12.11.113
57. Anwar, Talha, Poom Kumam, Zahir Shah, Wiboonsak Watthayu, and Phatiphat Thounthong. "Unsteady radiative natural convective MHD nanofluid flow past a porous moving vertical plate with heat source/sink." *Molecules* 25, no. 4 (2020): 854. https://doi.org/10.3390/molecules25040854
58. Siddiqui, Bushra Khatoon, Samina Batool, Qazi mahmood ul Hassan, and M. Y. Malik. "Repercussions of homogeneous and heterogeneous reactions of 3D flow of Cu-water and AL2O3-water nanofluid and entropy generation estimation along stretching cylinder." *Ain Shams Engineering Journal* 13, no. 1 (2022): 101493. https://doi.org/10.1016/j.asej.2021.05.007